Increased ^{18}F-FDG uptake on PET/CT is associated with poor arterial and portal perfusion on multiphase CT in patient with hepatocellular carcinoma

Sang Hyun Hwang

Department of Medicine

The Graduate School, Yonsei University

Increased ^{18}F-FDG uptake on PET/CT is associated with poor arterial and portal perfusion on multiphase CT in patient with hepatocellular carcinoma

Directed by Professor Mijin Yun

The Master's Thesis
submitted to the Department of Medicine,
the Graduate School of Yonsei University
in partial fulfillment of the requirements for the degree
of Master of Medical Science

Sang Hyun Hwang

June 2016

This certifies that the Master's Thesis of
Sang Hyun Hwang is approved.

Thesis Supervisor : Mijin Yun

Thesis Committee Member#1 : Kyung Sik Kim

Thesis Committee Member#2 : Joon Seok Lim

The Graduate School
Yonsei University

June 2016

ACKNOWLEDGEMENTS

First of all, I would like to express my gratitude to Professor Mijin Yun, who is my thesis director. Her encouragement, guidance and support in every step of the process enable me to develop an understating of the subject.

Also, I am indebted to Professor Kyung Sik Kim, and Joon Seok Lim, for their help on pertinent advice to assure superior quality of this paper.

I owe my gratitude to Professor Won Jun Kang and Arthur Cho, for helpful suggestions that gave inspiration to this paper.

Especially, I would likely to give my special thanks to my parents and to my brother who always support me.

<TABLE OF CONTENTS>

LIST OF FIGURES

LIST OF TABLES

ABSTRACT

Increased ^{18}F-FDG uptake on PET/CT is associated with poor arterial and portal perfusion on multiphase CT in patient with hepatocellular carcinoma

Sang Hyun Hwang

Department of Medicine
The Graduate School, Yonsei University

(Directed by Professor Mijin Yun)

Purpose: To correlate ^{18}F-FDG uptake on PET/CT with patterns of arterial and portal perfusion on multi-detector CT (MDCT) in patients with hepatocellular carcinoma (HCC) and to assess the value of variables from PET/CT and MDCT in predicting histological grades and overall survival.

Methods: We retrospectively analyzed MDCT and PET/CT of 66 patients with HCC who underwent surgical treatment. Tumor peak standard uptake value (SUV) was divided by the mean liver SUV (T/L_{SUV}). The mean tumor Hounsfield unit (HU) to mean liver HU was calculated for arterial (T/L_{HU-A}) and portal phases (T/L_{HU-P}). All patients were divided into three groups: I, $T/L_{HU-A} \leq 1$ and $T/L_{HU-P} < 1$; II, $T/L_{HU-A} > 1$ and $T/L_{HU-P} < 1$; and III, $T/L_{HU-A} > 1$ and $T/L_{HU-P} \geq 1$. The relationships between the CT perfusion groups and T/L_{SUV} were assessed. Multivariate logistic regression analyses were performed using clinical and imaging parameters for predicting histological grade. Overall survival curves stratified by T/L_{SUV} and CT perfusion groups were estimated using the Kaplan-Meier method.

Results: Statistically significant differences in T/L_{SUV} were noted between groups I and II (2.29 [range 1.74-3.60] vs. 1.20 [range 1.07-1.58], $p<0.001$) and groups I and III (2.29 [range 1.74-3.60] vs. 1.30 [range 1.07-1.43], $P<0.001$). In multivariate analysis, a T/L_{SUV} cut-off of >1.46 was the only independent predictor of tumor grade, with an odds ratio of 8.462 (95% confidence interval 1.799-39.803). Kaplan-Meier curves showed significant differences in OS according to T/L_{SUV} >1.62, group I perfusion pattern, and T/L_{SUV} >1.62 plus group I perfusion pattern (P=0.04, P=0.021, and P=0.002, respectively).

Conclusion: ^{18}F-FDG PET/CT is not commonly used for detecting HCC due to its limited sensitivity. We found that increased ^{18}F-FDG uptake is associated with decreased arterial and portal perfusion on MDCT. This can be used to preselect patients who would benefit the most from PET/CT. Meanwhile, ^{18}F-FDG uptake remained as the only independent predictor of histological grade, and higher ^{18}F-FDG uptake and lower perfusion pattern on MDCT were significantly related to shorter OS.

Key words: hepatocellular carcinoma, 18F-fluorodeoxyglucose, positron emission tomography, perfusion, metabolism

Increased ^{18}F-FDG uptake on PET/CT is associated with poor arterial and portal perfusion on multiphase CT in patient with hepatocellular carcinoma

Sang Hyun Hwang

Department of Medicine
The Graduate School, Yonsei University

(Directed by Professor Mijin Yun)

I. INTRODUCTION

Hepatocellular carcinoma (HCC) is the most common type of primary liver malignancy in adults, ranking as the third most common cause of cancer-related death worldwide [1]. When the clinical context is appropriate, characteristic features on conventional multiphase computed tomography (CT) or magnetic resonance imaging (MRI) are considered diagnostic of HCC in the absence of tissue biopsy [2]. Advanced imaging techniques, such as perfusion CT or MRI, have been used for further characterization of HCC (e.g., quantitative evaluation of tumor angiogenesis) [3]. Among imaging modalities, CT shows better linear correlation between the concentration of contrast material in tissue and contrast enhancement than MRI [4-6]. Despite this advantage, the use of CT perfusion imaging is limited due to high radiation exposure [7]. Meanwhile, enhancement parameters on routine multiphase CT have been shown to be well correlated with angiogenesis on histology [8].

Positron emission tomography/computed tomography (PET/CT) using fluorine-18-fluorodeoxyglucose (^{18}F-FDG) is a non-invasive method used to assess tumor-related glycolysis, a prominent metabolic phenotype in cancer. Although most malignant tumors show increased ^{18}F-FDG uptake, certain tumors, including HCC, renal cell carcinomas, and prostate cancers, are

notorious for low ^{18}F-FDG uptake on PET/CT, limiting its usefulness [9-13]. Meanwhile, perfusion is reported to affect tumor metabolism [14], and investigators have assessed correlations between CT perfusion and ^{18}F-FDG uptake on PET/CT in several types of cancers, but not HCC [15-20].

In this study, we aimed to analyze the relationship between ^{18}F-FDG uptake on PET/CT images and patterns of arterial and portal perfusion on multi-detector CT (MDCT) images in patients with hepatocellular carcinoma (HCC), as they may be of use in selecting individuals who could benefit the most from PET/CT. We also assessed the clinical value of variables derived from PET/CT and CT in predicting histological grades which are not routinely obtained in standard staging and overall survival.

II. MATERIALS AND METHODS

1. Patients

We retrospectively enrolled 74 patients diagnosed with HCC who underwent MDCT and ^{18}F-FDG PET/CT for preoperative staging from April 2008 to December 2012 at our hospital. Following exclusion of eight patients who underwent prior treatment for HCC before MDCT or PET/CT, 66 patients (51 male, 15 female, mean age 56.9 ± 11.0 years old) were left for analysis. The HCCs included ranges in size from 2.0 cm to 15.0 cm (mean 4.3 ± 2.5 cm). For patients with multiple lesions, we analyzed the largest tumor only. The average interval between MDCT and PET/CT was 11.7 ± 6.9 days. The mean duration of clinical follow-up was 43.0 ± 20.0 months (range 0.0-87.8 months). Our Institutional Review Board approved this retrospective study, and the requirement for informed consent was waived.

2. CT protocol

CT scans were performed with a second-generation dual source CT

system (SOMATOM Definition Flash, Siemens Healthcare, Forchheim, Germany). All scans were performed after injection of body weight (kg) x 2 ml of the intravenous contrast Ultravist (iopromide, Bayer HealthCare, Montville, New Jersey) at a rate of 3-4 ml/sec. Hepatic arterial phase CT (HAP-CT) scanning was performed 18 seconds after enhancement in the abdominal aorta reached 100 Hounsfield units (HU) for 5 seconds. Portal venous phase CT (PVP-CT) scanning was performed 30 seconds after the end of arterial phase scanning. The acquisition parameters were 128 x 0.6 mm detector collimation and 0.5 sec gantry rotation. Tube voltage and tube current were calculated automatically by CARE kV and CARE Dose 4D (Siemens Healthcare) with reference values of 120 kV and 170mAs, respectively. Using this system, we identified optimized settings for tube voltage and tube current based on each patient's topogram and reference settings. Slice thickness and increments were set at 5 mm each.

3. PET/CT protocol

All patients fasted for at least 6 hours and had blood glucose concentrations of less than 140 mg/dl before undergoing injection with ^{18}F-FDG. Approximately 5.5 MBq of ^{18}F-FDG per kilogram of body weight was administered intravenously. PET/CT scanning was performed from the skull base to the mid-thigh 60 minutes after injection in a three-dimensional mode at 2 minutes per bed position, using a dedicated PET/CT scanner (Discovery 600, General Electric Medical Systems, Milwaukee, WI, USA). Low-dose CT was performed using the following parameters: a scout view at 10 mA and 120 kVp, followed by a spiral CT scan with a 0.8-s rotation time, 60 mA, 120 kVp, 3.75-mm section thickness, 1.25-mm collimation, and 27.5-mm table feed per rotation with arms raised. CT images were reconstructed onto a 512 x 512 matrix, and were converted into 511 keV equivalent attenuation factors for attenuation correction. PET images were reconstructed onto a 128 x 128 matrix using

ordered subset expectation maximization and corrected for random and scatter coincidences.

4. Imaging and data analysis

CT and PET/CT images were retrospectively reviewed and analyzed on a dedicated workstation by two radiologists and two nuclear medicine physicians. All images were analyzed using the commercially available imaging software MIM (MIM-6.4, MIM software Inc., Cleveland, OH, USA). First, PET and HAP or PVP CT images were registered using a fusion module in MIM. The maximal ^{18}F-FDG uptake (SUVmax) and its location were obtained within the tumor volume on CT. Tumor peak SUV was obtained for a spherical ROI of 1cm diameter centered at the maximum ^{18}F-FDG uptake point. We determined background liver SUV values by drawing three 1cm diameter spherical regions of interest (ROIs) in the normal liver, two in the right lobe and one in the left lobe. The peak SUV of the tumor was divided by the mean SUV of background liver (T/L_{SUV}). SUV was calculated as follows: SUV = (decay-corrected activity [kBq] per ml of tissue volume)/(injected ^{18}F-FDG activity [kBq]/body weight [g]). In CT image analysis, the same ROIs for tumor and normal liver were copied on the fused HAP or PVP CT images. The mean HU values were measured from each ROI and the ratio of mean tumor HU to the mean HU of the liver was calculated for arterial (T/L_{HU-A}) and portal phases (T/L_{HU-P}).

5. Statistical analysis

The following variables were included in statistical analysis: age, gender, tumor size, the number of tumor nodules, serum alpha fetoprotein (AFP) level, T/L_{HU-A}, T/L_{HU-P}, and T/L_{SUV}. Tumor grade was categorized as low (Edmondson-Steiner grade I and II) or high (Edmonson-Steiner grade III and IV).

With a T/L_{HU-A} cutoff of >1 and a T/L_{HU-P} cutoff of <1, all patients were

divided into three groups: group I, $T/L_{HU-A} \leq 1$ and $T/L_{HU-P} < 1$; group II, $T/L_{HU-A} > 1$ and $T/L_{HU-P} < 1$; and group III, $T/L_{HU-A} > 1$ and $T/L_{HU-P} \geq 1$. There were no patients showing $T/L_{HU-A} \leq 1$ and $T/L_{HU-P} \geq 1$. The relationships between three CT perfusion groups and T/L_{SUV} on PET/CT were assessed by Kruskal-Wallis test and Dunn's post hoc analysis.

Univariate logistic regression analyses were performed to evaluate the relationships between each of the predictor variables, including age, gender, tumor size, the number of tumor nodules, serum AFP, T/L_{HU-A}, T/L_{HU-P}, and T/L_{SUV}, as well as histological grade as a dependent variable. The multicollinearity between variables was evaluated by calculating Spearman's rank correlation coefficient before the multivariate analysis. All continuous variables except serum AFP were grouped into two categories according to specific cut-off values determined by receiver-operating characteristic (ROC) curve analysis. In multivariate logistic regression analysis, only independent variables with $p < 0.05$ in univariate analysis were included. Kaplan–Meier survival analyses stratified by T/L_{SUV}, CT perfusion pattern, and T/L_{SUV} plus CT perfusion pattern were performed to calculate cumulative overall survival (OS). Survival time was calculated from the time from surgical resection to death or last follow-up visit at our hospital. All analyses were performed using SPSS software version 20.0 (IBM Corp., Armonk, NY, USA). Statistical significance was defined by a P-value <0.05 for all statistical analyses.

III. RESULTS

Patient demographics are summarized in Table 1. When all patients were grouped according to CT perfusion patterns, there were 15 patients (22.7%) in group I, 31 (47%) in group II, and 20 (30.3%) in group III. Increased arterial and decreased portal perfusion was the most frequent perfusion pattern in this study. The median T/L_{SUV} was 2.29 (interquartile range 1.74-3.60) in group I, 1.20 (interquartile range 1.07-1.58) in group II, 1.30 (interquartile range 1.07-1.43) in group III. When the CT perfusion groups were analyzed with T/L_{SUV} on PET/CT, the mean values of T/L_{SUV} were significantly different among the three groups ($P<0.001$). Dunn's post hoc test showed statistically significant differences in T/L_{SUV} between groups I and II and groups I and III ($P<0.001$ for both) (Fig. 1). HCCs with decreased arterial and portal perfusion (group I perfusion pattern) showed increased ^{18}F-FDG uptake on PET/CT (Fig. 2).

In contrast, there was no difference in T/L_{SUV} between groups II and III. Both groups II and III had a T/L_{HU-A} cutoff of >1; however, group II comprised a T/L_{HU-P} cutoff of <1 and group III had a T/L_{HU-P} cutoff of ≥1. Regardless of the amount of portal perfusion, a T/L_{HU-A} cutoff of >1 was associated with low ^{18}F-FDG uptake that could not be distinguished from the surrounding liver (Figs. 3 and 4). As a result, our study confirmed that the degrees of ^{18}F-FDG uptake in HCCs are significantly correlated with arterial rather than portal perfusion.

Table 1. Patient demographics

Characteristic		Total(n=66)
Age at diagnosis(yr)		Median: 55(range: 29-81)
Gender		
	Male	49(74.2%)
	Female	17(25.8%)
Tumor size(cm)		4.3±2.5(median: 3.6; range: 2.0-15.0)
Tumor number		
	Single	57(86.4%)
	Multiple	9(13.6%)
Serum ‖AFP(ng/mL)		Median: 28.03(range: 1.65-120000)
BCLC staging		
	A	62(93.9%)
	B	4(6.6%)
†T/L_{HU-A}		1.32±0.38(median: 1.31; range: 0.65-2.41)
‡T/L_{HU-P}		0.91±0.18(median 0.93; range: 0.50-1.36)
§T/L_{SUV}		1.65±0.88(median 1.32; range: (0.68-4.88)

‖AFP = α-fetoprotein, †T/L_{HU-A} = the ratio of tumor HU to the mean HU of the liver at arterial phase, ‡T/L_{HU-P} = the ratio of tumor HU to the mean HU of the liver at portal phase, §T/L_{SUV} = the ratio of tumor SUVpeak to the mass SUV of the liver.

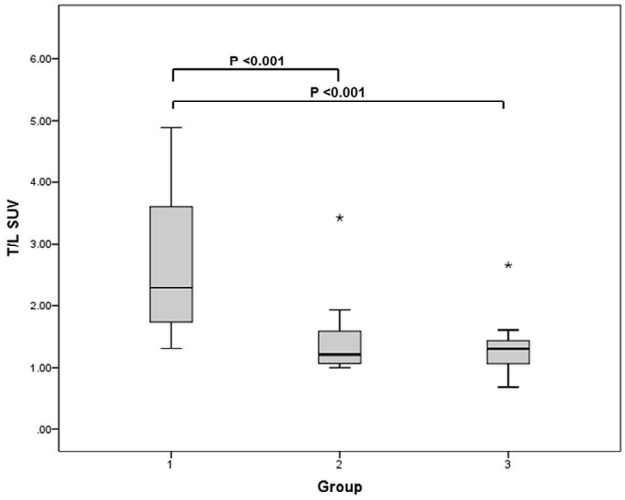

Fig. 1 Side-by-side box plots of T/L_{SUV} according to each CT perfusion group. Kruskal-Wallis test and Dunn's posthoc analysis show statistically significant differences between groups I and II and groups I and III ($P < 0.001$, for both) (group I: $T/L_{HU\text{-}A} \leq 1$ and $T/L_{HU\text{-}P} < 1$, group II: $T/L_{HU\text{-}A} > 1$ and $T/L_{HU\text{-}P} < 1$, group III: $T/L_{HU\text{-}A} > 1$ and $T/L_{HU\text{-}P} \geq 1$).

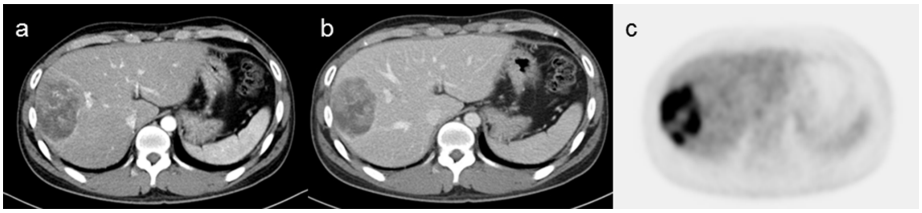

Fig. 2 Axial images on arterial (A) and portal phases (B) of CT and PET/CT (C) for an HCC with group I perfusion ($T/L_{HU\text{-}A} \leq 1$ and $T/L_{HU\text{-}P} < 1$). The mass shows decreased arterial and portal perfusion on CT, but increased ^{18}F-FDG uptake on PET/CT.

Fig. 3 Axial images on arterial (A) and portal phases (B) of CT and PET/CT (C) for an HCC with group II perfusion ($T/L_{HU\text{-}A} > 1$ and $T/L_{HU\text{-}P} < 1$). The mass shows increased arterial perfusion and decreased portal perfusion on CT and demonstrates ^{18}F-FDG uptake similar to adjacent hepatic parenchyma on PET/CT.

Fig. 4 Axial images on arterial (A) and portal phases (B) of CT and PET/CT (C) for an HCC with group III perfusion ($T/L_{HU\text{-}A} > 1$ and $T/L_{HU\text{-}P} \geq 1$). The mass shows increased arterial perfusion and preserved portal perfusion on CT and demonstrates ^{18}F-FDG uptake similar to adjacent hepatic parenchyma on PET/CT.

There were 30 low-grade HCCs and 36 high-grade HCCs on pathologic evaluation. Table 2 summarizes the results of the univariate and multivariate logistic regression analyses of age, gender, tumor size, the number of tumor nodules, serum AFP level, T/L_{HU-A}, T/L_{HU-P}, and T/L_{SUV} as independent variables and HCC histological grade as a dependent variable. In univariate analyses, tumor size, T/L_{HU-A}, T/L_{HU-P}, and T/L_{SUV} were found to be significant for predicting histological grades, with T/L_{SUV} having the lowest P-value ($P<0.001$). In multivariate analysis, the T/L_{SUV} cut-off of >1.46 remained as the only independent predictor of tumor grade, with an odds ratio of 8.462 (95% confidence interval, 1.799-39.803).

Table 2. Relationship between clinical, imaging parameters and histological grade

Variables	No. of patients with High grade	Univariate analysis OR(95% *CI)	P-value	Multivariate analysis OR(95% *CI)	P-value
Age (yr)			0.063		
>66	4/13	Reference			
≤66	32/53	3.429(0.934-12.581)			
Gender			0.332		
Male	25/49	Reference			
Female	11/17	1.760(0.562-5.512)			
Tumor size			0.004		0.137
>3.5cm	24/33	4.667(1.643-13.256)		2.558(0.741-8.828)	
≤3.5cm	12/33	Reference		Reference	
Tumor number			0.052		
Single	34/57	Reference			
Multiple	2/9	0.193(0.037-1.015)			
Serum ‖AFP		1.001(1.000-1.002)	0.137		
†T/L_{HU-A}			0.01		0.479
High(>1.38)	9/26	Reference		Reference	
Low(≤1.38)	27/40	3.923(1.381-11.147)		1.601(0.435-5.898)	
‡T/L_{HU-P}			0.003		0.730
High(>0.85)	18/44	Reference		Reference	
Low(≤0.85)	18/22	6.500(1.883-22.437)		1.335(0.259-6.884)	
§T/U_{SUV}			<0.001		0.007
High(>1.46)	22/25	14.143(3.601-55.553)		8.462(1.799-38.803)	
Low(≤1.46)	14/41	Reference		Reference	

*CI = confidence interval, ‖AFP = α-fetoprotein, †T/L_{HU-A} = the ratio of tumor HU to the mean HU of the liver at arterial phase, ‡T/L_{HU-P} = the ratio of tumor HU to the mean HU of the liver at portal phase, §T/L_{SUV} = the ratio of tumor SUVpeak to the mass SUV of the liver.

During the mean follow-up of 43 months, 11 patients (16.7%) died of HCC. Kaplan-Meier curves showed significant differences in OS according to T/L_{SUV}>1.62, group I perfusion pattern, and T/L_{SUV}>1.62 plus group I perfusion pattern (5-year overall survival, 70% vs. 92.6%, P=0.04; 66.7% vs. 91.3%, P=0.021; and 58.3% vs. 91.8%, P=0.002, respectively). Higher ^{18}F-FDG uptake and lower perfusion on MDCT were significantly related to shorter OS (Fig. 5).

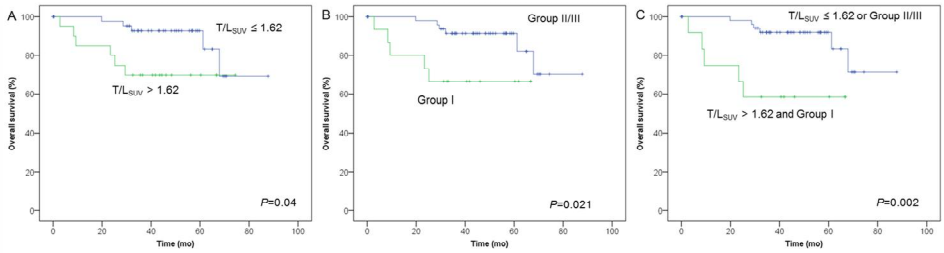

Fig. 5 Kaplan-Meier curves of OS according to T/L_{SUV} >1.62 (A), group I CT perfusion (B), and T/L_{SUV} >1.62 plus group I CT perfusion (C).

IV. DISCUSSION

Hemodynamic changes from a predominantly portal flow to a solely arterial flow are closely associated with multistep hepatocarcinogenesis. Portal flow is known to decrease at an early stage and further decrease as tumors progress [21]. High interstitial pressure due to increased vascular permeability of leaky, abnormal tumor vasculature and the absence of functional lymphatics within advanced tumors may contribute to the reversal of low-pressure portal flow from its usual direction [22]. Thereafter, instead of acting as feeding vessels for nutrients and supporting nearly half of the hepatic oxygen requirement, the portal veins become draining vessels for HCCs [23,24]. The resultant hypoxia and nutrient shortage related to the magnitude of portal flow reversal seem to contribute to angiogenesis in HCCs.

The evaluation of these hemodynamic changes has been the basis of

non-invasive detection methods and the characterization of premalignant or malignant hepatic nodules on CT and MRI [25-28]. Of the hepatic circulatory phases, the arterial phase represents the distribution of contrast material from the hepatic arterial blood. Hypervascular HCCs are best seen during this phase, since the hepatic parenchyma is yet to be fully enhanced due to the main blood supply from the portal veins. At the portal venous phase, the hepatic parenchyma shows peak contrast enhancement, whereas typical HCCs appear hypoattenuated due to the lack of blood supply from the portal veins. Data in the literature regarding correlation between angiogenesis and glucose metabolism in HCC are limited. Kitamura et al. observed predominant GLUT-1 expression in relatively hypoxic areas, suggesting a negative association between glucose metabolism and angiogenesis. They also found that Ki-67, a proliferative marker, was positively associated with ^{18}F-FDG uptake on PET [29]. The results suggested outgrowth of tumor over perfusion.

In this study, we found the association between perfusion patterns on multiphase CT and degrees of ^{18}F-FDG uptake on PET/CT. As long as arterial perfusion was increased, changes in portal perfusion alone were insufficient to increase ^{18}F-FDG uptake. In contrast, arterial decompensation in spite of decreased portal perfusion was associated with increased ^{18}F-FDG uptake in HCCs. The insufficient arterial perfusion seems attributable to slower proliferation of endothelial cells than rapidly growing neoplastic cells [14,30,31]. The resultant increase of intercapillary distance would make rapid growing tumors to be less angiogenic than slow growing ones. Accordingly, hypoxia inducible factor-1 (HIF-1), a transcriptional factor stimulated in response to insufficient angiogenesis, increases glycolytic flux and the metastatic potential of tumors [14,32]. Thus, the extraction of more glucose per perfusion to overcome insufficient angiogenesis seems one of the mechanisms related to increased ^{18}F-FDG uptake in HCCs.

The above findings may hold important clinical implications. So far,

there is no definite clinical or imaging factor that can predict ^{18}F-FDG uptake in HCCs. Using the perfusion patterns on multiphase CT, patients who would show increased ^{18}F-FDG uptake in their HCCs can be preselected, reducing false negative PET/CT studies for staging intrahepatic tumors and distant metastases. Secondly, studies have shown lower objective response rates to trans-arterial chemoembolization in HCCs with a higher T/L_{SUV}. According to our results, less effective drug delivery resulting from poor arterial perfusion in HCCs with high ^{18}F-FDG uptake might have contributed to the finding [31,33,34]. Further investigations are needed to determine whether the restoration of tumor perfusion may enhance responses to chemotherapy by ameliorating insufficient perfusion and improving drug distribution in HCCs with a higher T/L_{SUV}.

A diagnosis of HCC can be made according to flow characteristics on CT or MRI with appropriate clinical context. However, information on histological grade cannot be obtained by this approach. A few reports have shown the value of ^{18}F-FDG uptake for predicting histological differentiation and aggressiveness in HCCs [12,13,35,36]. In addition, different treatment responses and patient survival outcomes are reportedly associated with degrees of ^{18}F-FDG uptake in primary tumors [33,34]. In this study, we found a T/L_{SUV} cutoff of >1.46 to be the only significant predictor of poor histological grade. More importantly, Kaplan-Meier curves showed significant differences in OS according to T/L_{SUV}>1.62, group I perfusion pattern, and T/L_{SUV}>1.62 plus group I perfusion pattern. Higher ^{18}F-FDG uptake and lower perfusion on MDCT were significantly related to shorter OS. Despite low sensitivity in detecting primary tumors and metastases, ^{18}F-FDG uptake in primary tumors could hold value for non-invasive prediction of histological grade, treatment response, and patient prognosis.

There are a few limitations that warrant consideration in this study. First, we used multiphase MDCT instead of perfusion CT. Accordingly, there might be some variability in scan delay for the arterial phase after contrast injection. Also, since arterial phase imaging is affected more by scan timing than portal phase

imaging [37], the results of T/L_{HU-A} may be less accurate than those of T/L_{HU-P} using multiphase CT, compared to perfusion CT. Second, the HCCs in this study were all 2 cm in size or larger. Therefore, it is unknown whether or not the relationships between arterial and portal perfusion patterns and ^{18}F-FDG uptake that we observed in our study are also present in smaller HCCs.

V. CONCLUSION

In HCC ≥2 cm, increased ^{18}F-FDG uptake on PET/CT was associated with decreased arterial and portal perfusion on CT. The perfusion patterns on CT may help to avoid false negative scans and to preselect patients who could benefit the most from ^{18}F-FDG PET/CT. Also, our findings suggest that cytotoxic chemotherapies that consider vascularization strategies could improve drug delivery in HCCs with high ^{18}F-FDG uptake. Lastly, we found that ^{18}F-FDG uptake was an independent predictor of histological tumor grade, and higher ^{18}F-FDG uptake and lower perfusion on MDCT were significantly related to shorter OS.

REFERENCES

1. Ferlay J, Shin HR, Bray F, Forman D, Mathers C, Parkin DM. Estimates of worldwide burden of cancer in 2008: GLOBOCAN 2008. Int J Cancer 2010;127:2893-917.
2. Bruix J, Sherman M. Management of hepatocellular carcinoma: an update. Hepatology 2011;53:1020-2.
3. Hennedige T, Venkatesh SK. Imaging of hepatocellular carcinoma: diagnosis, staging and treatment monitoring. Cancer Imaging 2013;12:530-47.
4. Goh V, Padhani AR. Imaging tumor angiogenesis: functional assessment using MDCT or MRI? Abdom Imaging 2006;31:194-9.
5. Chen Y, Zhang J, Dai J, Feng X, Lu H, Zhou C. Angiogenesis of renal cell carcinoma: perfusion CT findings. Abdom Imaging 2010;35:622-8.
6. Taouli B, Johnson RS, Hajdu CH, Oei MT, Merad M, Yee H, et al. Hepatocellular carcinoma: perfusion quantification with dynamic contrast-enhanced MRI. AJR Am J Roentgenol 2013;201:795-800.
7. Ippolito D, Capraro C, Casiraghi A, Cestari C, Sironi S. Quantitative assessment of tumour associated neovascularisation in patients with liver cirrhosis and hepatocellular carcinoma: role of dynamic-CT perfusion imaging. Eur Radiol 2012;22:803-11.
8. Kim YI, Chung JW, Park JH, Kang GH, Lee M, Suh KS, et al. Multiphase contrast-enhanced CT imaging in hepatocellular carcinoma correlation with immunohistochemical angiogenic activities. Acad Radiol 2007;14:1084-91.
9. Oyama N, Akino H, Suzuki Y, Kanamaru H, Sadato N, Yonekura Y, et al. The increased accumulation of [18F] fluorodeoxyglucose in untreated prostate cancer. Japanese journal of clinical oncology 1999;29:623-9.
10. Ho C-L, Simon C, Yeung DW. 11C-acetate PET imaging in

hepatocellular carcinoma and other liver masses. Journal of Nuclear Medicine 2003;44:213-21.

11. Kang DE, WHITE Jr RL, Zuger JH, Sasser HC, Teigland CM. Clinical use of fluorodeoxyglucose F 18 positron emission tomography for detection of renal cell carcinoma. The Journal of urology 2004;171:1806-9.
12. Khan MA, Combs CS, Brunt EM, Lowe VJ, Wolverson MK, Solomon H, et al. Positron emission tomography scanning in the evaluation of hepatocellular carcinoma. J Hepatol 2000;32:792-7.
13. Park JW, Kim JH, Kim SK, Kang KW, Park KW, Choi JI, et al. A prospective evaluation of 18F-FDG and 11C-acetate PET/CT for detection of primary and metastatic hepatocellular carcinoma. J Nucl Med 2008;49:1912-21.
14. Cairns RA, Harris IS, Mak TW. Regulation of cancer cell metabolism. Nature Reviews Cancer 2011;11:85-95.
15. Goh V, Engledow A, Rodriguez-Justo M, Shastry M, Peck J, Blackman G, et al. The flow-metabolic phenotype of primary colorectal cancer: assessment by integrated 18F-FDG PET/perfusion CT with histopathologic correlation. J Nucl Med 2012;53:687-92.
16. Groves AM, Wishart GC, Shastry M, Moyle P, Iddles S, Britton P, et al. Metabolic-flow relationships in primary breast cancer: feasibility of combined PET/dynamic contrast-enhanced CT. Eur J Nucl Med Mol Imaging 2009;36:416-21.
17. Bisdas S, Spicer K, Rumboldt Z. Whole-tumor perfusion CT parameters and glucose metabolism measurements in head and neck squamous cell carcinomas: a pilot study using combined positron-emission tomography/CT imaging. AJNR Am J Neuroradiol 2008;29:1376-81.
18. Miles KA, Griffiths MR, Keith CJ. Blood flow-metabolic relationships are dependent on tumour size in non-small cell lung cancer: a study

using quantitative contrast-enhanced computer tomography and positron emission tomography. Eur J Nucl Med Mol Imaging 2006;33:22-8.

19. Tateishi U, Nishihara H, Tsukamoto E, Morikawa T, Tamaki N, Miyasaka K. Lung tumors evaluated with FDG-PET and dynamic CT: the relationship between vascular density and glucose metabolism. J Comput Assist Tomogr 2002;26:185-90.
20. Abramyuk A, Wolf G, Shakirin G, Haberland U, Tokalov S, Koch A, et al. Preliminary assessment of dynamic contrast-enhanced CT implementation in pretreatment FDG-PET/CT for outcome prediction in head and neck tumors. Acta Radiol 2010;51:793-9.
21. Kudo M. Imaging blood flow characteristics of hepatocellular carcinoma. Oncology 2002;62:48-56.
22. Carmeliet P, Jain RK. Angiogenesis in cancer and other diseases. Nature 2000;407:249-57.
23. Tochio H, Kudo M, Okabe Y, Morimoto Y, Tomita S. Association between a focal spared area in the fatty liver and intrahepatic efferent blood flow from the gallbladder wall: evaluation with color Doppler sonography. AJR Am J Roentgenol 1999;172:1249-53.
24. Vollmar B, Menger MD. The hepatic microcirculation: mechanistic contributions and therapeutic targets in liver injury and repair. Physiological reviews 2009;89:1269-339.
25. Foley WD, Mallisee TA, Hohenwalter MD, Wilson CR, Quiroz FA, Taylor AJ. Multiphase hepatic CT with a multirow detector CT scanner. AJR Am J Roentgenol 2000;175:679-85.
26. Kanematsu M, Goshima S, Kondo H, Nishibori H, Kato H, Yokoyama R, et al. Optimizing scan delays of fixed duration contrast injection in contrast-enhanced biphasic multidetector-row CT for the liver and the detection of hypervascular hepatocellular carcinoma. J Comput Assist

Tomogr 2005;29:195-201.

27. Kitao A, Zen Y, Matsui O, Gabata T, Nakanuma Y. Hepatocarcinogenesis: multistep changes of drainage vessels at CT during arterial portography and hepatic arteriography--radiologic-pathologic correlation. Radiology 2009;252:605-14.

28. McEvoy SH, McCarthy CJ, Lavelle LP, Moran DE, Cantwell CP, Skehan SJ, et al. Hepatocellular carcinoma: illustrated guide to systematic radiologic diagnosis and staging according to guidelines of the American Association for the Study of Liver Diseases. Radiographics 2013;33:1653-68.

29. Kitamura K, Hatano E, Higashi T, Narita M, Seo S, Nakamoto Y, et al. Proliferative activity in hepatocellular carcinoma is closely correlated with glucose metabolism but not angiogenesis. J Hepatol 2011;55:846-57.

30. Torimura T, Sata M, Ueno T, Kin M, Tsuji R, Suzaku K, et al. Increased expression of vascular endothelial growth factor is associated with tumor progression in hepatocellular carcinoma. Human pathology 1998;29:986-91.

31. Park YN, Kim Y-B, Yang KM, Park C. Increased expression of vascular endothelial growth factor and angiogenesis in the early stage of multistep hepatocarcinogenesis. Archives of pathology & laboratory medicine 2000;124:1061-5.

32. Potente M, Gerhardt H, Carmeliet P. Basic and therapeutic aspects of angiogenesis. Cell 2011;146:873-87.

33. Song MJ, Bae SH, Lee SW, Song do S, Kim HY, Yoo Ie R, et al. 18F-fluorodeoxyglucose PET/CT predicts tumour progression after transarterial chemoembolization in hepatocellular carcinoma. Eur J Nucl Med Mol Imaging 2013;40:865-73.

34. Kim BK, Kang WJ, Kim JK, Seong J, Park JY, Kim do Y, et al. 18F-fluorodeoxyglucose uptake on positron emission tomography as a prognostic predictor in locally advanced hepatocellular carcinoma. Cancer 2011;117:4779-87.

35. Delbeke D, Martin WH, Sandler MP, Chapman WC, Wright JK, Jr., Pinson CW. Evaluation of benign vs malignant hepatic lesions with positron emission tomography. Arch Surg 1998;133:510-5; discussion 5-6.

36. Seo S, Hatano E, Higashi T, Hara T, Tada M, Tamaki N, et al. Fluorine-18 fluorodeoxyglucose positron emission tomography predicts tumor differentiation, P-glycoprotein expression, and outcome after resection in hepatocellular carcinoma. Clin Cancer Res 2007;13:427-33.

37. Goshima S, Kanematsu M, Kondo H, Yokoyama R, Miyoshi T, Nishibori H, et al. MDCT of the liver and hypervascular hepatocellular carcinomas: optimizing scan delays for bolus-tracking techniques of hepatic arterial and portal venous phases. AJR Am J Roentgenol 2006;187:W25-32.

ABSTRACT(IN KOREAN)

간세포암에서 다중 컴퓨터단층촬영의 동맥, 정맥기에 조영되는 정도와 FDG 섭취 정도와 관련이 있음을 연구함

<지도교수 윤미진>

연세대학교 대학원 의학과

황상현

연구목적: 간세포암 환자에서 수술 전 시행한 전산화단층촬영의 동맥기 및 정맥기 영상에서 관찰되는 관류 양상과 양전자방출단층촬영에서 관찰되는 ^{18}F-FDG 섭취 정도와의 관련성을 규명하고, 이 검사들로 얻은 인자로부터 병리등급 및 예후와 관계를 규명하고자 하였다.

대상 및 방법: 2008년 4월부터 2012년 12월까지 세브란스병원에서 간세포암을 진단받고, 치료 전 병기결정을 위해 전산화단층촬영 및 양전자방출단층촬영술 시행 후 수술 한 66명의 환자를 대상으로 하였다. 간세포암과 정상간의 표준섭취계수(SUV)의 비율(T/L_{SUV}), 하운스필드 단위(HU) 비율을 동맥기(T/L_{HU-A}) 및 정맥기(T/L_{HU-P})에서 각각 측정하였다. 전산화단층촬영의 동맥기 및 정맥기에서 관찰되는 양상에 따라서 각각의 군으로 나누었다. 1군은 $T/L_{HU-A} \leq 1$ 및 $T/L_{HU-P} < 1$ 이며, 2군은 $T/L_{HU-A} > 1$ 이며 $T/L_{HU-P} < 1$, 3군은 $T/L_{HU-A} > 1$ 이며 $T/L_{HU-P} \geq 1$ 에 해당한다. 각 군에서 T/L_{SUV}의 차이를 비교하였으며 또한 이러한 영상검사에서 얻은 인자들과 임상 인자들과 병리등급간의 관계를 분석하였으며, T/L_{SUV} 및 전산화단층촬영에서

관찰되는 양상으로 분류한 군을 이용하여 생존율을 분석하였다.

결과: T/L_{SUV}는 1군과 2군 (2.29 [1.74–3.60] vs. 1.20 [1.07–1.58], P < 0.001) 및 1군과 3군 (2.29 [1.74–3.60] vs. 1.30 [1.07–1.43], P < 0.001)에서 통계학적으로 표준섭취계수(SUV)가 유의미한 차이가 있었다. 다변량분석에서 T/L_{SUV}만이 유일하게 병리 등급을 예측할 수 있었다. Kaplan-Meier 생존분석에서 T/L_{SUV} >1.62인 군, 1군, 및 T/L_{SUV} >1.62 이며 1군을 동시에 만족하는 환자 군에서 그렇지 않은 군과의 생존율이 각각 유의미한 차이를 나타내었다 (P = 0.04, P = 0.021, P = 0.002).

결론: 간세포암에서 ^{18}F-FDG 섭취 증가는 전산화단층촬영의 동맥기 및 정맥기에서 관류 감소와 관계가 있으며 이는 양전자방출단층촬영이 유용할 수 있는 간세포암 환자를 미리 알 수 있는데 도움이 될 수 있다. 또한 ^{18}F-FDG 섭취 정도는 수술 전 병리 등급을 알 수 있는 유일한 인자이며 높은 ^{18}F-FDG 섭취 및 낮은 관류는 간세포암에서 좋지 않은 예후를 나타낸다.

핵심되는 말 : 간세포암, 양전자방출단층촬영술, ^{18}F-FDG, 물질대사

PUBLICATION LIST

Hwang SH, Lee M, Lee N, Park S, Kim CK, Park MA, et al. Increased 18F-FDG Uptake on PET/CT is Associated With Poor Arterial and Portal Perfusion on Multiphase CT. Clin Nucl Med 2016;41:296-301.